Research Article
Open Access
CrossMark

"Pompon" graphene as a new promising anode for LIBs

Abstract

The "pompon" graphene was obtained by the new modified controlled detonation gas synthesis tested as an anode of LIBs. Processing of Raman spectra by changing the position of the G-band shows the presence of a mixture of 2, 3 and 4-layer graphene structures. The results of the surface area measurement by the BET method have been shown the limited availability of the "pompons" for the penetration of lithium ions between its layers. Subsequent thermomechanical activation leads to partial "delamination" of the pompon and the production of both separate and 2-layer sheets of graphene, which is reflected in a sharp increase in its specific surface area. The specific capacity of graphene, as an anode of LIBs, increases in the range M0 < M20 < M40 and reaches of 500 mAh•g^{-1} at a current density of 37.2 mA•g^{-1} for the best M40 sample. The obtained values of specific capacity are 1.5 times higher than similar values for graphite-based anodes.

Keywords: pompon graphene, lithium-ion battery

Volume 7 Issue 1 - 2023

O.V. Potapenko,[1,2] K.Vavilon,[2] V. Zinin,[3] H. Potapenko,[1,2] Zhang Qian,[1] Shengwen Zhong[1]
[1]Jiangxi University of Science and Technology, China
[2]Ningbo IPMS Research and Technology Center Co Ltd, China
[3]Ukrainian State University of Chemical Technology, Ukraine

Correspondence: O.V. Potapenko, Jiangxi University of Science and Technology, 86 Hongqi Avenue, Zhanggong District, Ganzhou, Jiangxi, PR, China, Tel +380666607963, E mail 1978hikin@gmail.com

Received: February 13, 2023 | **Published:** March 14, 2023

Introduction

Global climate change has led to an increase in demand for renewable energy resources, as the use of fossil fuels causes irreparable harm to the environment. Renewable energy solutions can meet the daily needs of consumers, while reducing the consumption of fossil fuels and ensuring efficient energy consumption.

Graphene is a new generation material that finds potential and practical application in various fields of research. The mechanical and physic -chemical properties of graphene and the subsequent variety of its applications paved the way for new opportunities in the future for a variety of devices and systems. Graphene has unsurpassed characteristics, mainly in terms of electronic conductivity, mechanical strength and large surface area, which makes it possible to achieve outstanding results in the field of materials science.[1] Graphene-based derivatives, such as functionalized GO and rGO modifications of graphene, are widely used as catalysts in "green" hydrogen energy,[2] and also find application in various types of batteries.

Due to its improved thermal conductivity, graphene is also an excellent material for achieving advanced heat distribution solutions that include radiators or films use for heat dissipation.[3] In addition, the special structural and morphological characteristics and the greatest ratio of the surface area to the volume, graphene have plenty advancement for application in energy storage batteries and supercapacitors.[4] One such example is a Li-C battery[5–9] combining a lithium intercalation electrode in the anode and a capacitive electrode in the cathode to achieve energy density at the battery level in combination with the specific power of super capacitor. Compared with graphite, the traditional anode material in LIBs, graphene has a higher theoretical capacity of 740 mAh•g-1, since Li ions can be adsorbed on both sides of the graphene sheet, forming the C3Li intercalates.[10]

Experimentally, a practical capacity value of 672 mA h g^{-1} for a graphene anode was achieved, which indicates great prospects for its use, both in pure form and as part of composites with graphite, silicon, etc.

In this paper, we consider the behavior of the new type of "pompon" graphene as a LIB anode. It should be noted that this paper the behavior of "pompon" graphene in its pure form is considered, unlike earlier papers,[11] where the use of lithium particles or foil on the anode side, including graphene, is proposed.

Materials and methods

As an object of research, "pompon" graphene M0, obtained by the method of chemical vapor deposition (CVD), as well as its modifications M20 and M40, differing from pure graphene by mechanical grinding for 20 and 40 minutes accompanied by intensive heating of the sample, were used. Raman microscopy and transmission electron microscopy methods were applied to confirm the structure of the resulting graphenes. Micro-Raman spectra were measured in geometry for reflection at room temperature using a triple Raman spectrometer T-64000 Horiba Jobin-Yvon (Japan). Laser lines with a wavelength of 532.0 nm were used for excitation. The radiation was focused on the sample applying the 50x/NA 0.75 lens into a spot with a diameter of ~ 1 micron. The laser radiation power on the sample was ~1 MW. The obtained spectra were normalized to the intensity of the G-band for ease of perception. M0, M20 and M40 graphene samples were placed on a CaF_2 substrate in a dry form, and then large aggregated parts were removed by air flow. The force of the air flow was selected so that individual non-aggregated micro particles of the sample remained on the substrate. The points for spectral investigation were randomly selected within the region of a uniformly deposited sample or individual micro particles (Figure 1).

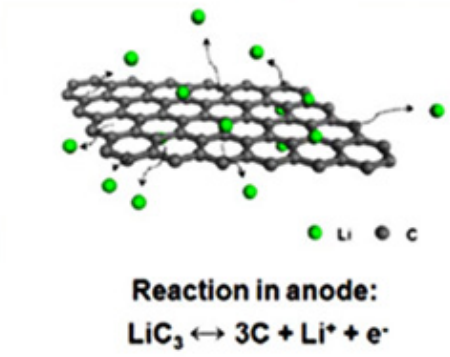

Figure 1 Diagram of the reaction of lithium ions on the surface of a graphene sheet (www.nature.com/scientificreports/DOI: 10.1038/srep05278).

Electrochemical tests of graphene-based anodes were carried out in CR2016 coin cells. The electrode mass was prepared by mixing "pompon" graphene and a water-soluble binder NV-1T in the 85:15 ratios. The resulting suspense was covered to the copper foil by a Doctor Blade applicator. The thickness of the material layer was ≈30 μm. The manufactured electrodes were dried in vacuum at the 120-130 ºC upon several hours. 1M $LiPF_6$ solution in a mixture of EC: DMC (1:1) (Sigma Aldrich) as an electrolyte, lithium metal as an opposite electrode, and the Celguard 2500 as the separator were used. All operations for assembling coin cells were carried out in the dry argon box. Electrochemical measurements of the samples were carried out in the range of potentials ΔE = 0.01 - 3.0 V (rel. Li+/Li) using the electrochemical workstation Autolab (Netherlands) and the electrochemical impedance was studied by the 2-electrode circuit scheme and analyzed by the NOVA software.

Results and discussion

Physico-chemical properties

In Figure 2 the Raman spectra and TEM micrographs of "pompon" graphenes are presented. For all samples, D, G and 2D bands of the sp^2 phase of carbon (disordered graphene or nanographite) are recorded at ~1350, ~1580 and ~2700 cm^{-1}.

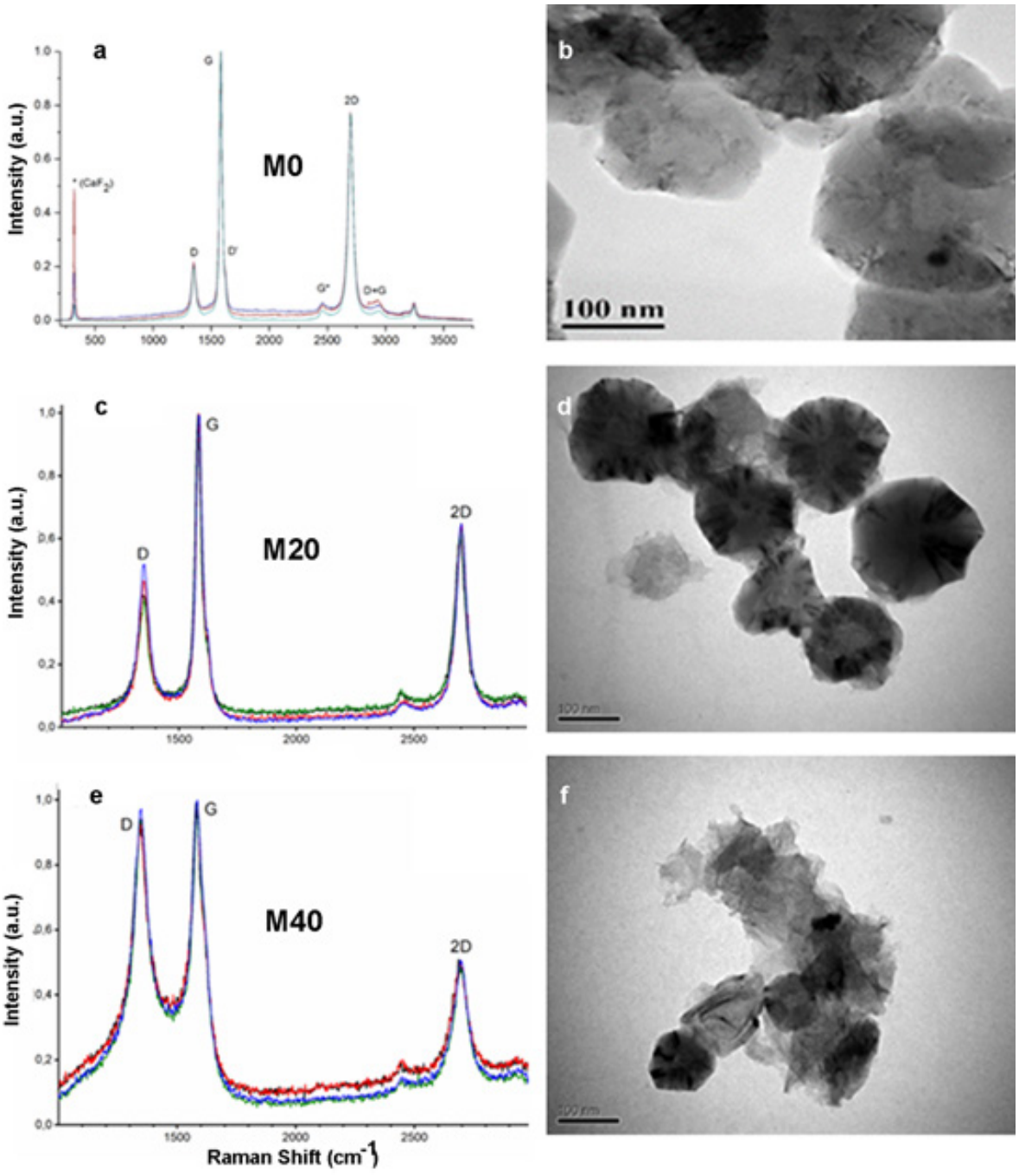

Figure 2 Raman spectra and SEM images of "pompon" graphenes: M0 (a, b), M20 (c, d), M40 (e,f).

Citation: Potapenko OV, Vavilon K, Zinin V, et al. "Pompon" graphene as a new promising anode for LIBs. *Material Sci & Eng.* 2023;7(1):23–26.
DOI: 10.15406/mseij.2023.07.00198

The Raman spectra of the graphene show two bands. The first is at 1350 cm^{-1}, and another two G- and 2D-bands registry at 1580 and 2650 cm^{-1}. The G-band is caused by valence vibrations of the sp^2 bonds of the graphite structure, while the D-band is associated with structural disordering (structural defects).[12]

The band at 1350 cm^{-1} is assigned to the D-band, which is associated with a double resonance (DR) Raman process from the transverse optical modes of K-point phonons of A1g symmetry in a structural defect or disordered structures of the sp^2 domains in graphene nanostructure in part. The slight peak at 1610 cm^{-1} is named the D'-band that observes via a double resonance process due to the defects. The sharp G-band at 1580 cm^{-1} corresponds to an optical E^2g phonon at the Brillouin Zone center of all sp^2 hybridized carbons, while 2D-band at 2700 cm^{-1} corresponds to overtones of the D-band. This band is present even in absence of defects because it is the sum of two phonons with opposite momentum. The high intensity of the two-phonon 2D-band of the second order in graphene is conditioned by the process of double electron-phonon resonance, and the shape of the band itself reflects the structure of electronic zones in the vicinity of the K-point of the Brillouin zone (single contour for single-layer graphene, four-component for two-layer graphene, and two-component for graphite crystal).

As we talked above, the appearance of a clear D-band while maintaining a relatively large I2D/IG intensity ratio is typical for graphene containing structural defects.[12] For the M40 sample, wider D, G and 2D-bands are recorded, as well as a more intense D-band (ID/IG = 1.3÷1.5) in comparison with other samples, which generally indicates a greater degree of sp^2 disordering, which is characteristic of graphene oxide,[13,14] and this indicates that partial sp2 domains are not restored completely at different levels for M40 sample.

Hence, it can be concluded that intensive mechanical processing of pompon graphene, accompanied by intensive heating in the air, leads to its partial oxidation.

The calculation of the number of graphene layers by changing the position of the G-bands was carried out according to the method presented in.[15] To more accurately determine the position of the maximum, the characteristic spectral region was approximated by peaks with the shape of the Lorentz contour. The results of analyses of various areas of the sample show the predominant presence of 2, 3 and 4-layer graphenes.

Analyzing micrographs of various types of graphene, it can be noted that the "pompom" consisting of several layers of graphene "unfolds" with the formation of separate sheets during thermomechanical processing. It should be noted that the number of individual graphene leaves increases, and the sizes of pompons themselves decrease with increasing processing time. This is clearly noticeable if we compare the micrographs of the initial graphene (M0) and the graphene after thermomechanical activation (M20 and M40). And it is in good agreement with the degree of disordered layers determined by the R=ID/IG ratio of intensities.

The results are obtained correlate well with the change in the specific surface area of graphene using the BET method. In Figure 3 the histogram of changes of these values for various graphene modifications is presented. Thus, for M0, M10, M20 and M40 samples the surface area values are 28.23 $m2 \cdot g^{-1}$, 233.9 $m2 \cdot g^{-1}$, 314.5 $m2 \cdot g^{-1}$, 474 $m2 \cdot g^{-1}$, accordingly.

Taking into account the fact that a larger number of individual graphene leaves are observed during machining for 40 minutes, and this modification has the largest specific surface area, we assumed that M40 graphene-based electrodes would be more "accessible" for the introduction of lithium ions and have higher electrochemical parameters.

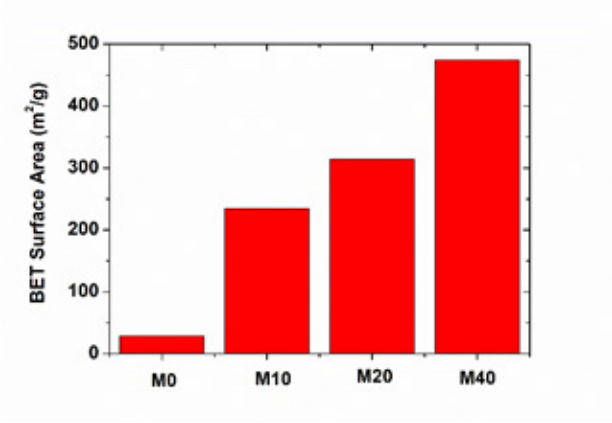

Figure 3 Changing the specific surface area of various graphene modifications.

Electrochemical properties

The charge-discharge curves for graphene-based electrodes are presented in Figure 4. The final charge and discharge voltage for them is 3.0 V and 0.01 V, accordingly, the charge/discharge current is 37.2 $mA \cdot h^{-1}$. The dependence the capacity of the different modifications graphenes on the number of cycle is shown in Figure 5.

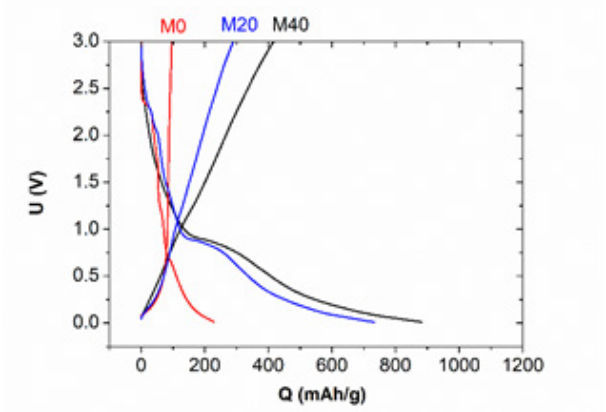

Figure 4 Charge/discharge curves on the 1-st cycle of the graphene-based anode material.

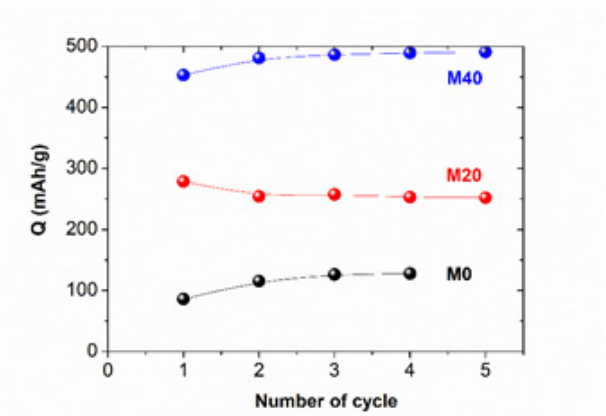

Figure 5 Change in the discharge specific capacity of graphenes upon cycling.

Citation: Potapenko OV, Vavilon K, Zinin V, et al. "Pompon" graphene as a new promising anode for LIBs. *Material Sci & Eng.* 2023;7(1):23–26.
DOI: 10.15406/mseij.2023.07.00198

During the primary intercalation of lithium into graphene, the process of formation of the SEI film can be observed on the curves, which is in the range of potentials 0.9 – 0.4 V (rel. Li+/Li). Below 0.4 V, the process of adsorption of lithium ions into the structure of the material occurs, which can be compatible with the intercalation processes.

The specific capacity of various types of graphene during the desorption of lithium ions varies in the range M40 > M20> M0, which correlates well with the change in the specific surface area of materials. Based on changes in the specific capacity of materials, electrochemical cycling of graphene M40 was performed at various current loads Using an anode material of this composition, it is possible to note an irreversible loss of specific capacity on the 1-st cycle, which leads to a low coulombic efficiency of about 50%. Further cycling of the graphene electrode leads to a decrease in the specific capacity of the material and an increase in its coulombic efficiency.

It should be noted that the specific capacity of graphene M40 at low charge/discharge currents is about 500 mAh/g, which significantly exceeds the values characteristic of graphite anodes. An increase in the charge currents of the material leads to decreasing in the specific capacity, and at current equal to 372 $mA \bullet g^{-1}$ the specific capacity is below 200 $mAh \bullet g^{-1}$. The subsequent reduction of charge/discharge currents to 186 mA/g leads to an increase in the specific capacity, however, its original values are not restored completely. This effect may be associated with an irreversible mechanism of lithium accumulation at the interface of graphene nanosheets and electrolyte.[16]

Thus, in our paper we have shown that the graphene we have obtained is a promising anode material for renewable power sources. Among the advantages are the following:

a) Ease and simplicity of obtaining graphenes

b) The obtained high values of specific capacitance in comparison with other anode materials

c) Cycling stability, which indicates the absence of significant degradation of the material during operation as an anode for LIBs.

Conclusions

The "pompon" graphene is obtained by the new modified controlled detonation gas synthesis tested as an anode of LIBs. Using the Raman spectroscopy data by changing the position of the G-band, the presence of the mixture of 2,3 and 4-layer graphenes has been observed. The surface area measurement by the BET method prove that the limited availability of the pompons for the penetration of lithium ions between their layers. In consequence of the following thermomechanical activation, the partial "delamination" of pompons and the production of both separate and 2-layer sheets of graphene, which is reflected in a sharp increase in its specific surface area. The specific capacity of graphene, as an anode for LIBs, increases in the range M0 < M20 < M40, and reaches of 500 $mAh \bullet g^{-1}$ at a current density of 37.2 $mA \bullet g^{-1}$ for the M40 sample, respectively. The obtained values of specific capacity for pompon graphenes are 1.5 times higher than values for graphite-based anodes. This fact creates very good prospects for use this material both in "pure" form and as a conductive matrix for other electrode compositions.

Acknowledgments

None.

Funding

None.

Conflicts of interest

There are no conflicts of interest.

References

1. Wei D, Kivioja J. Graphene for energy solutions and its industrialization. *Nanoscale*. 2013;5:10108–10126.
2. Iqra S, Syed AA, Tokeer. Graphene-based derivatives heterostructured catalytic systems for sustainable hydrogen energy via overall water splitting. *Catalysts*. 2023;13:109.
3. Balandin A. Toward ubiquitous environmental gas sensors-capitalizing on the promise of graph graphene. *Nature Materials*. 2011;10:569–581.
4. El Kady MF, Shao Y, Kaner RB. Graphene for batteries, supercapacitors and beyond. *Nature Reviews Materials*. 2016;1(7):16033–16046.
5. Simon P, Gogotsi Y, Dunn B. Where do batteries end and super capacitors begin? *Science*. 2014;343:1210–1211.
6. Kim JH, Kim JS, Lim YG, et al. Effect of carbon types on the electrochemical properties of negative electrodes for Li-ion capacitors. *J Pow Sour*. 2011;196:10490–10495.
7. Sivakkumar SR, Pandolfo AG. Evaluation of lithium-ion capacitors assembled with pre-lithiated graphite anode and activated carbon cathode. *Electrochimica Acta*. 2012;65:280–287.
8. Du Pasquier A, Plitz I, Menocal S, et al. A comparative study of Li ion battery, super capacitor and nonaqueous asymmetric hybrid devices for automotive applications. *Journal Power Sources*. 2003;115:171–178.
9. Park MS, Lim YG, Kim JH, et al. A novel lithium-doping approach for an advanced lithium ion capacitor. *Advanced Energy Materials*. 2011;1:1002–1006.
10. Wang G, Wang B, Wang X, et al. Sn/graphene nanocomposite with 3D architecture for enhanced reversible lithium storage in lithium ion batteries. *Journal of Materials Chemistry*. 2009;19(44):8378–8384.
11. Jang BZ, Liu C, Neff D, et al. Graphene surface-enabled lithium ion-exchanging cells: next generation high-power energy storage devices. *Nano Letters*. 2011;11(9):3785–3791.
12. Ferreira M, Marcus EH, Moutinho VO, et al. Evolution of the raman spectra from single-few and many-layer graphene with increasing disorder. *Physical Review B*. 2010;82(12):125429–125437.
13. Childres I, Jauregui LA, Park W, et al. Raman spectroscopy of graphene and related materials. *New Developments in Photon and Materials Research*. 2013;1:1–20.
14. Kostiuk D, Bodik M, Siffalovic P, et al. Reliable determination of the few-layer graphene oxide thickness using raman spectroscopy. *Journal of Raman Spectroscopy*. 2016;47(4):391–394.
15. Wang H, Wang Y, Cao X, et al. Vibrational properties of graphene and graphene layers. *Journal of Raman*. 2009;40(12):1791–1796.
16. Pan D, Wang S, Zhao B, et al. Li storage properties of disordered graphene nanosheets. *Chemistry of Materials*. 2009;21(14):3136–3142.

Citation: Potapenko OV, Vavilon K, Zinin V, et al. "Pompon" graphene as a new promising anode for LIBs. *Material Sci & Eng*. 2023;7(1):23–26.
DOI: 10.15406/mseij.2023.07.00198